Pellicle choice for 193-nm immersion lithography photomasks

Eric Cotte[a]*, Rüdiger Häßler[b]**, Benno Utess[a], Gunter Antesberger[a],
Frank Kromer[a], and Silvio Teuber[a]
[a]Advanced Mask Technology Center (AMTC), Rähnitzer Alle 9, 01109 Dresden (Germany)
[b]Institut für Polymerforschung Dresden (IPF-DD), Hohe Strasse 6, 01069 Dresden (Germany)

ABSTRACT

An assessment of the mechanical performance of pellicles from different vendors was performed. Pellicle-induced distortions were experimentally measured and numerical simulations were run to predict what improvements were desirable. The experiments included mask registration measurements before and after pellicle mounting for three of the major pellicle suppliers, and adhesive gasket material properties characterization for previously untested samples. The finite element numerical simulations were verified via comparison to experimental data for pellicles with known frame bows, measured by the vendor. The models were extended to simulate the effect of the chucking of reticles in an exposure tool, as well as the various magnification correction schemes available in such tools. Results were compared to ITRS requirements to evaluate performances. This study enables the AMTC to give important feedback to pellicle suppliers and make proper recommendations to customers for future pellicle choices.

Keywords: pellicle, distortions, photomask, gasket, frame flatness, mechanical testing.

1. INTRODUCTION

The main goal of pellicles is to prevent particles from falling on the absorber pattern and printing, but pellicles have experimentally been shown to introduce pattern distortions.[1,2] This should be of concern to lithographers, in addition to other considerations such as pellicle transmission and cleanliness.[3] Pellicle-induced distortions studies exist in the literature, combining experimental and numerical results, but refinements were needed.[4-10] Indeed, these distortions become more of an issue as the extension of 193 nm immersion lithography down to smaller nodes implies that pellicles will continue being used while image placement requirements are tightened.

The distortions caused by the specific pellicles from different vendors used at the AMTC, namely MLI, Mitsui, and INKO, were evaluated in detail. In the rest of the paper, the vendors will not be named and will only be referred to as A, B and C for confidentiality reasons. Similarly, dimensions and material properties will not be mentioned explicitly in order to prevent vendor identification. For all vendors, the pellicle dimensions were available and most material properties could be found in the past publications.[4-9] Input data that had not previously been reported, such as the gasket material properties for Vendor A, was determined experimentally. The latter was performed at the Institut für Polymerforschung Dresden (IPF-DD), using a Dynamic Mechanical Analyzer to obtain the elastic modulus of the material.

Then, experimental registration data was obtained to quantify the pellicle-induced distortions for unconstrained reticles. Using finite element modeling, the distortions pertaining to the pellicles tested experimentally were calculated for reticles chucked in an exposure tool, in which the constraints on the reticle are different from in a registration tool, and typical exposure tool image placement corrections were applied. Finally, the distortion residuals were compared to the ITRS requirements.[11]

*email: Eric.Cotte@amtc-dresden.com; **email: rhaesz@ipdfdd.de

Figure 1 is a schematic of a reticle and pellicle, on which the frame dimensions depend on the vendor and type of pellicle. Exact dimensions are not given for confidentiality reasons. Figure 2 is a side view of this same system, illustrating the heights of the Al pellicle frame and adhesive gasket used to attach the pellicle on a reticle. Finally, Table 1 lists the material properties and thicknesses of the pellicle / reticle system components for the various types available at the AMTC. Since one of the vendors' adhesive gasket properties had not been characterized, it had to be experimentally tested, as explained in the next section.

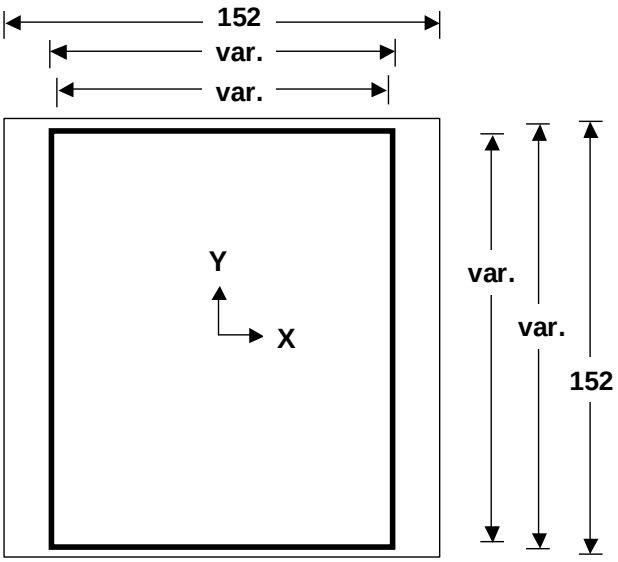

Fig. 1. Schematic of a reticle and typical pellicle. Dimensions in mm.

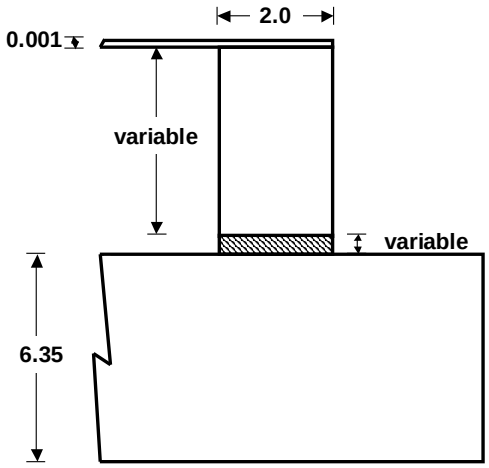

Fig. 2. Side view of a reticle and pellicle schematic showing the frame and gasket. Dimensions in mm.

Table 1. Material properties and thicknesses of the photomask and pellicle components.

Component	Material	Elastic modulus	Poisson's ratio	CTE (ppm/°C)	Thickness
Substrate	Quartz	72.6 GPa	0.16	0.55	6.35 mm
Absorber	Cr	248.0 GPa	0.30	12.0	80 mm
Frame	Al	72.0 GPa	0.33	23.6	3.7 to 6.0 mm
Adhesive	-	0.157 to 1.0 MPa	0.25	5.0	0.25 to 0.50 mm

2. MATERIAL PROPERTIES TESTING

A TA Instruments Dynamic Mechanical Analyzer (DMA) was used to measure the elastic modulus of adhesive gasket samples provided by vendor A. A photograph of the tool that was used at the Institut für Polymerforschung in Dresden is shown in Fig. 3. Modulus measurements with this tool are valid in a range of 10^3 Pa to 3×10^{12} Pa with a precision of ± 1%, which is suitable for the testing of this type of material. Samples are gripped between a fixed and a moving clamp and subjected to a known set of forces (or stresses), as shown in Fig. 4 (a), while their elongation (or their strain) is simultaneously measured. Figure 4 (b) illustrates the Poisson effect, i.e., the shrinking of the material in one direction while it is being strained in the orthogonal direction. It must be noted that this effect can only be visualized for high strains, well outside of the region of interest for the elastic modulus determination of pellicle gaskets. From the stress-strain curves thus obtained and shown in Fig. 5 (a), the elastic modulus can be measured as the slope of these curves in the appropriate stress or strain domain. Figure 5 (b) is a plot of the elastic modulus as a function of the applied strain. In the case of adhesive gaskets, the stresses applied on the gasket material once the pellicle is attached to the reticle are relatively small, so the elastic modulus of interest lies at the inception of the stress-strain curve, corresponding to a

minimum stress and strain state, as illustrated in Fig. 5 (c). As evidenced in Fig. 5 (b), the measured elastic modulus depends on the strain range considered, because the material's behavior is not simply elastic but visco-elastic. However, for low strains, there is a region where the elastic modulus is constant, and a value of 1.02 MPa was found for Vendor A gasket material.

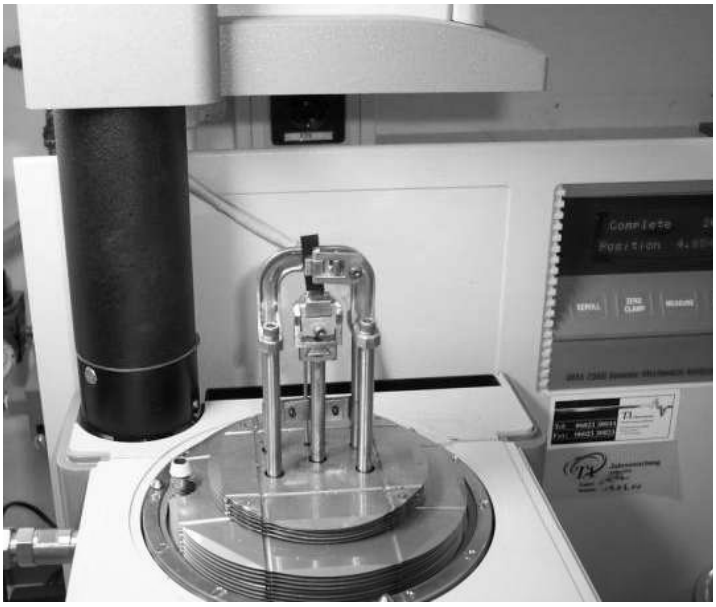

Fig. 3. Picture of a TA Instruments Dynamic Mechanical Analyzer with a pellicle gasket sample placed in the clamp.

(a) (b)

Fig. 4. Picture of a pellicle gasket sample in the DMA tension clamp for (a) low strain and (b) high strain loading conditions.

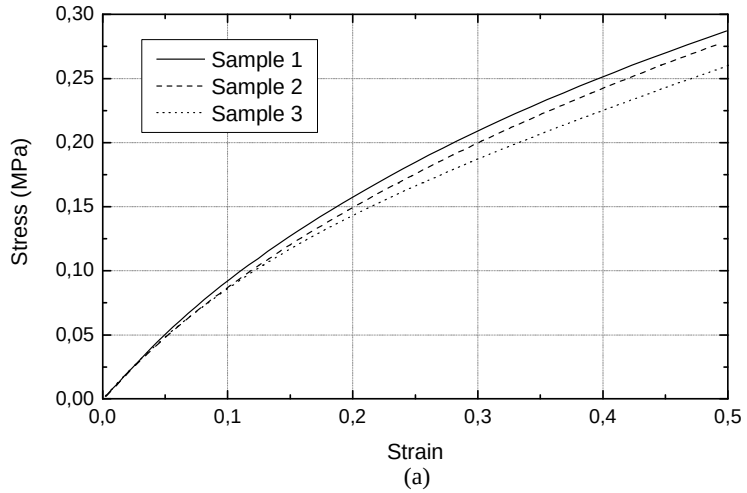

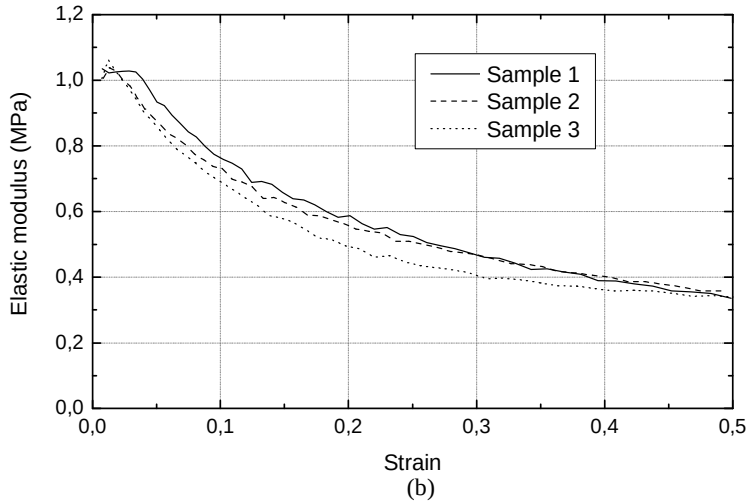

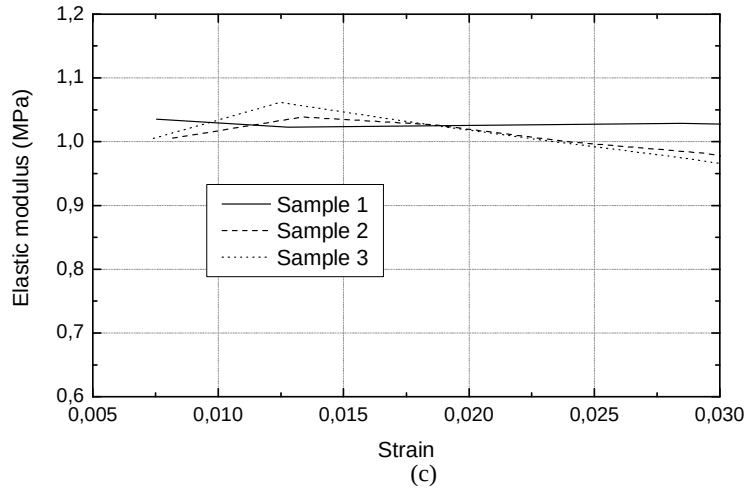

Fig. 5. (a) Stress-strain curves and plots of elastic modulus (b) for strains up to 50% and (c) in the low-strain region, for 3 adhesive gasket samples from Vendor A.

3. PELLICLE ATTACHMENT RESULTS

Reticle registration was measured before and after pellicle mounting to quantify pellicle-induced pattern displacement changes. Samples of one type of pellicle per vendor were experimentally tested in this manner. In parallel, finite element simulations were run for the same pellicle types, as well as a few more types from Vendor B. The models were benchmarked beforehand, using published results and pellicle samples with known frame bows. From the experimental pellicle-induced distortions, the initial bow of the frames was then determined using the models, providing a characterization of the pellicles. Figure 6 illustrates the numerically-calculated distortions due to pellicle mounting, plotted as lines of different colors and styles, as well as the experimental data for the tested pellicles, plotted as circles and using the same color schemes.

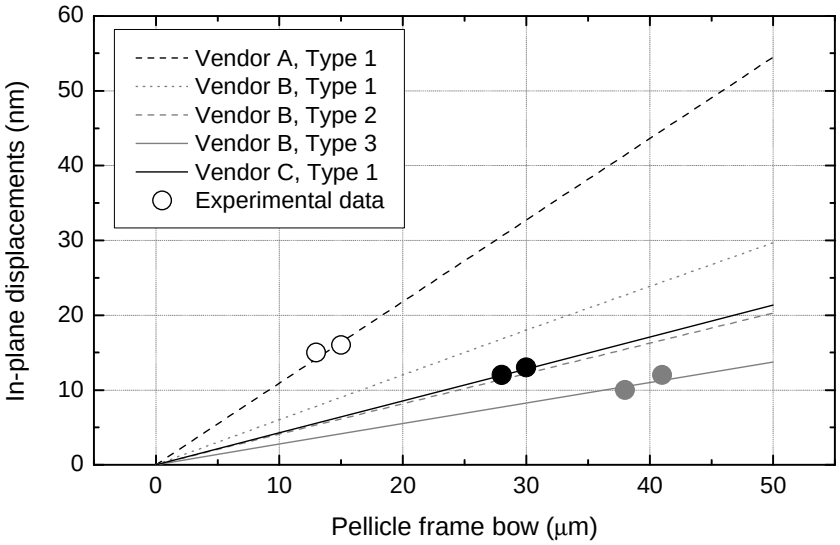

Fig. 6. Numerically- and experimentally-obtained pellicle-induced distortions as a function of the pellicle frame bow, for various vendors and pellicle types. Results pertain to an unconstrained reticle, as reported by a registration tool.

While each vendor had one gasket material to offer, various pellicle types were considered for Vendor B, differing in dimensions (length, width, and height of the pellicles), corresponding to the specific exposure tools they can be used in. The variations in pellicle frame stiffness due to the various dimensions are the reason behind the different distortions obtained for pellicles of Types 1, 2, and 3 from Vendor B. In essence, for a given gasket and frame bow, bowed frames with a smaller height induce less distortion, due to their lower stiffness. Additionally, for a fixed frame bow and set pellicle dimensions, pellicles with compliant gaskets induce smaller distortions than pellicles with stiffer gaskets. Finally, for fixed gasket types and pellicle dimensions, i.e., for different pellicle types, distortions are proportional to the pellicle frame bow. These rules of thumb also apply for the next results shown in this paper. It must be noted that pellicle vendors offer frames with different bow specifications, from 30 μm to 70 μm, but numerical results were plotted up to a value of 50 μm on all graphs to prevent identification of the respective vendors.

Allowable reticle image placement error requirements, as given by the ITRS, are not stated in terms of raw (or uncorrected) distortion data, but for magnification-corrected data.[11] Two main types of magnification correction are available: isotropic, which linearly corrects image placement with the same factor in two orthogonal directions, and orthotropic, which linearly corrects image placement with a different factor for two directions. For the 70 nm and 45 nm nodes, the ITRS requirements on mask image placement are 14.0 nm and 11.0 nm, respectively, after application of isotropic correction. In order to determine what portion of the error budget is taken up by the pellicle-induced distortions, isotropic magnification corrections were applied to the experimental and numerical data of Fig. 6, and the resulting residuals are plotted in Fig. 7. According to these results, pellicle-induced distortions could account for

anywhere between a third and two thirds of the error budget, depending on the node, pellicle vendor, and pellicle type considered. For example, pellicle mounting of a sample from Vendor C would cause 6.0 nm of distortions, leaving only 8.0 nm of the allowable image placement errors to other sources of photomask distortions at the 70 nm node.

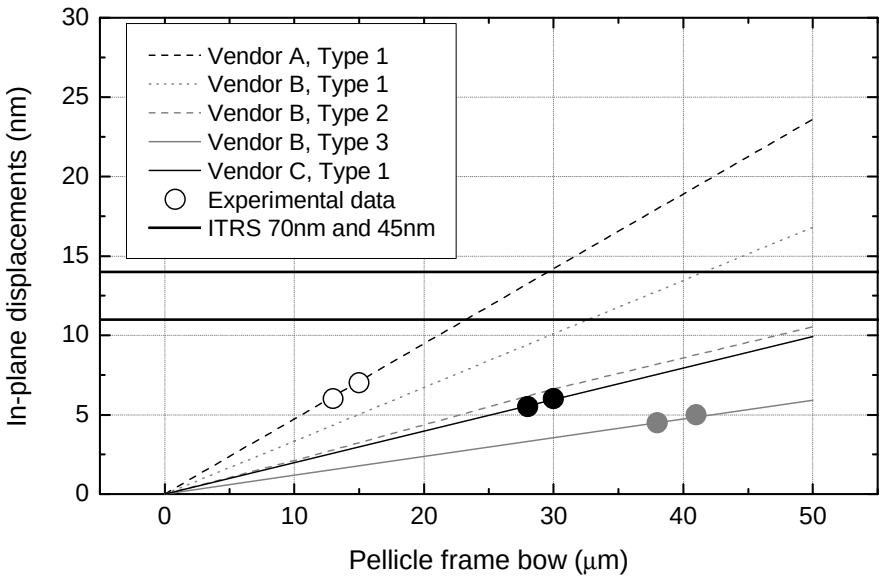

Fig. 7. Pellicle-induced distortions with isotropic corrections and comparison to ITRS specifications, for an unconstrained reticle.

But when if one considers that the image placement requirements are determined for mask-makers by chip-makers, it appears that this may not be the correct way to evaluate the contribution of pellicles to the mask distortions. Indeed, the numbers relating to image placement come from wafer printing tests, during which the mask is held in the exposure tool, clamped on the outside of the pellicle area and subjected to gravity, instead of being unconstrained. Therefore, the contribution of the chucking of the reticle in the exposure tool should be taken into account. This is discussed in the next section.

4. PHOTOMASK DISTORTIONS IN EXPOSURE TOOL

Figure 8 is a schematic illustrating the reticle orientation when held in the exposure tool, subjected to gravity and vacuum-chucked on either sides of the pellicle, with the pattern and pellicle facing down. The details of the regions of the reticle that are contacted by the exposure tool chuck are given in Fig. 9. Two extreme cases were considered, corresponding to a large chucked area and a small chucked area. In Fig. 9 (a), the largest possible area is used for chucking, which is considered a "best" case as it helps reduce the influence of gravity on reticle distortions. Conversely, Fig. 9 (b) depicts the "worst" case. For the following calculations, only the worst case was considered.

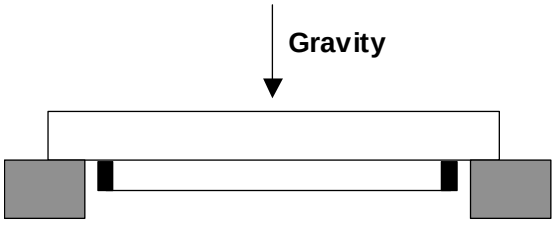

Fig. 8. Exposure tool reticle orientation (pellicle facing down), boundary conditions (chucked edges) and loading (gravity).

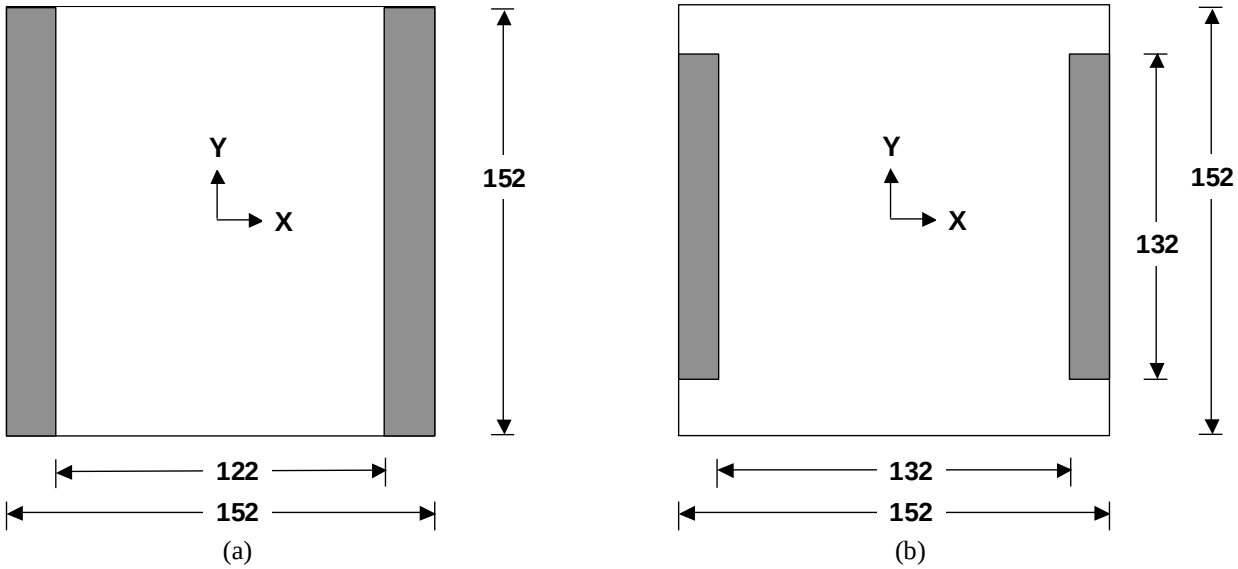

Fig. 9. Vacuum chucking areas (in grey) for a (a) best and (b) worst case exposure tool reticle chuck.

Figure 10 illustrates uncorrected pellicle-induced reticle distortions for a photomask chucked in an exposure tool, as shown in Fig. 9 (b). The results labeled as "experimental data" do not correspond to data obtained by measuring reticle registration in these conditions, as no printing tests were conducted, but to numerical predictions of these reticle in-plane distortions for the pellicle types and the specific frame bows determined in the previous section. Unlike for distortions measured in a registration tool, it is not possible to fully eliminate pellicle-induced effects by using flat frames, because the influence of gravity is not corrected for, unlike in the case of registration measurements, and the minimum distortions are 7.0 nm. An other difference with data from a registration tool is that pellicle-induced distortions for relatively large frame bows are smaller in the case of a reticle held in an exposure tool than in that of a reticle in a registration tool. This is due to the vacuum-chucking of the reticle on either side of the pellicle, which flattens the photomask and limits the effect of gravity, in turn reducing in-plane distortions.

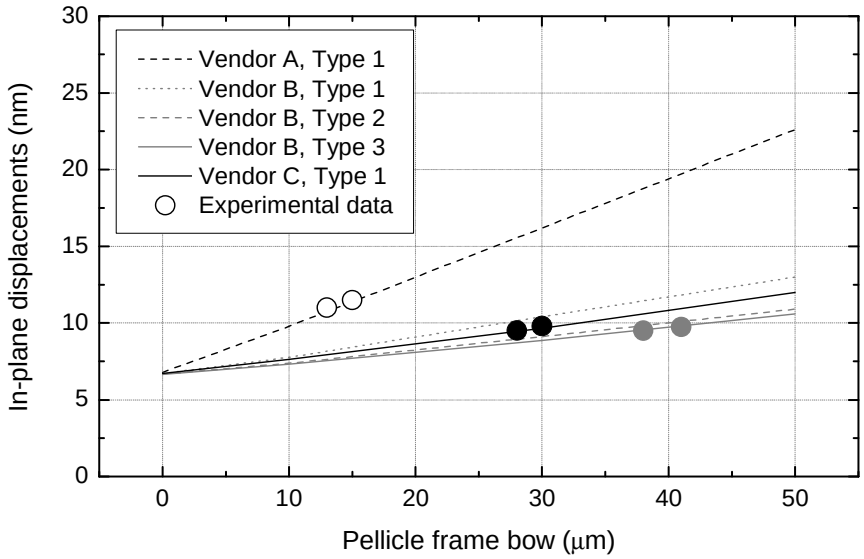

Fig. 10. Uncorrected numerical and experimental pellicle-induced distortions for a reticle in an exposure tool.

Figures 11 and 12 illustrate reticle distortions after the application of isotropic and orthotropic corrections, respectively. Orthotropic corrections perform much better than isotropic corrections, which barely reduce distortions below their raw values. While isotropic corrections are implied in the ITRS requirements on image placements, orthotropic corrections are common on most exposure tools and would thus be a better basis for the comparison of calculated image placement errors to specifications.

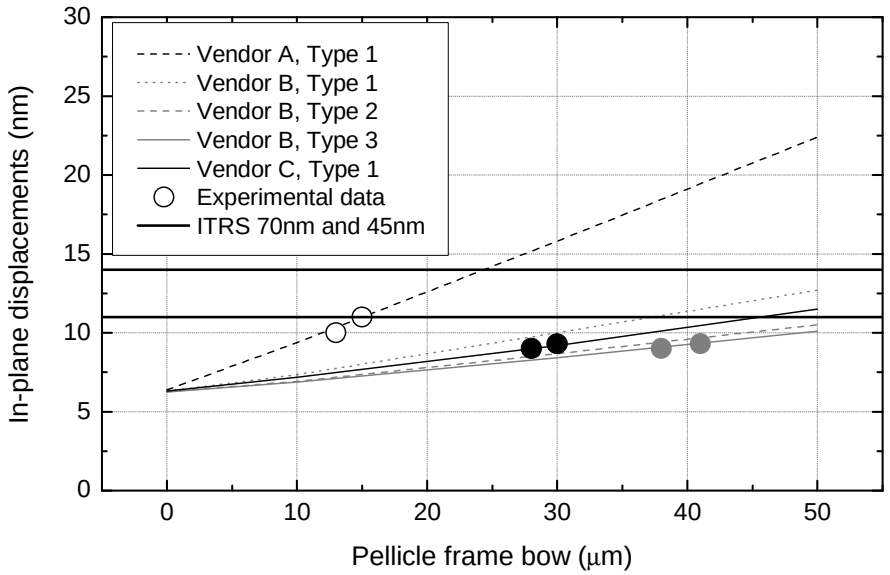

Fig. 11. Isotropically-corrected numerical and experimental pellicle-induced distortions for a reticle in an exposure tool.

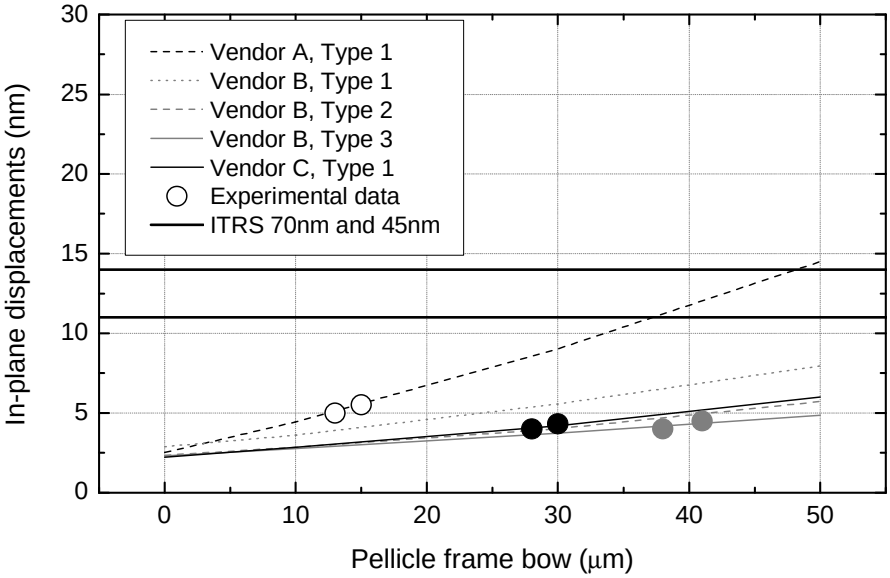

Fig. 12. Orthotropically-corrected numerical and experimental pellicle-induced distortions for a reticle in an exposure tool.

Figure 13 shows pellicle-induced distortions in an exposure tool after application of orthotropic corrections and removal of a 3rd order component in the x-direction, which is an option on some exposure tools. Distortions are lowered, and meeting the error budget appears more feasible.

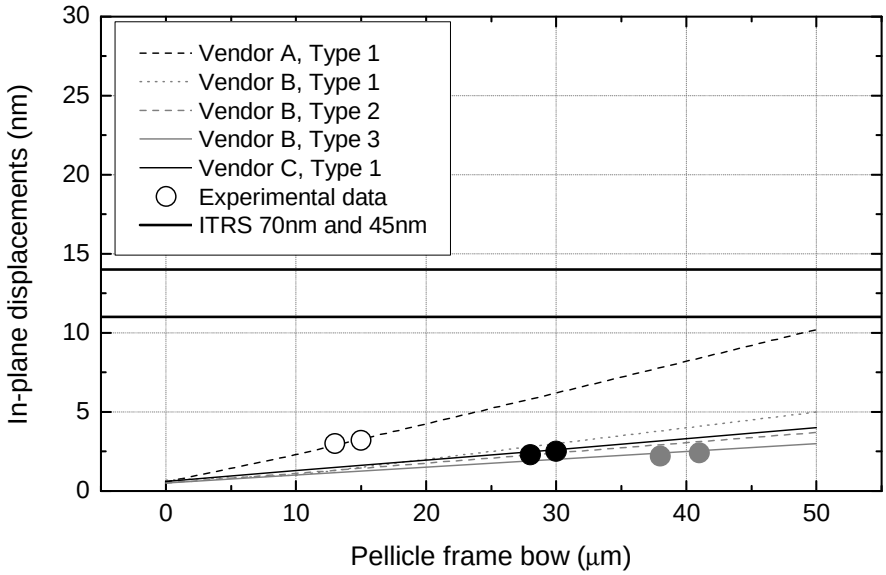

Fig. 13. Orthotropically- and 3rd order-corrected pellicle-induced distortions for a reticle in exposure tool. 3rd order correction implies the removal of a 3rd order term in the x-direction.

5. SUMMARY AND CONCLUSIONS

Pellicles from various vendors were fully characterized via determination of the missing material properties and estimation of the pellicle frame bow based on registration measurements. Models were built to calculate the pellicle-induced distortions of a reticle in an exposure tool, and magnification corrections were applied to mimic the capabilities of exposure tools.

A modification of the definition of the specification of mask image placement error in the ITRS documents is proposed, to better account for the fact that reticle in-plane distortions are different in a registration tool and in an exposure tool, as well as the fact that isotropic magnification correction is not the best scheme available in exposure tools. This might cause issues, because mask makers may not have the capability to measure registration for a reticle in an exposure tool or to model these distortions. In addition to this definition change, the following solutions are proposed to reduce the pellicle-induced distortions and enhance printing results:
(1) tighten internal specifications on pre-pelliclization photomask registration in order to meet the ITRS specifications once the reticle is held in printing conditions (chucked on both sides of the pellicle).
(2) use pellicles from a different vendor to minimize pellicle-induced distortions, although pellicle performances can be very close, depending on which specification is used. A further issue being that customers make pellicle choices based on many criteria, as mentioned in the literature.[3]
(3) reduce pellicle-induced distortions by suggesting that vendors make modifications to their pellicles. Modifications could include using more compliant gaskets, flatter frames, or slightly changing the size of pellicles if it does not cause issues in the exposure tool and the pellicle still keeps particles out of focus and prevents them from printing.

The understanding and reduction of pellicle-induced distortions is of significant importance due to the shrinking of error budgets that must accompany the successful application of dry 193 nm lithography and 193 nm immersion lithography.

ACKNOWLEDGMENTS

The authors would like to thank Claus Hense of DPI for his help during the realization of this project, and C. B. Wang of MLI for providing pellicle samples for the benchmarking of the models. The AMTC gratefully acknowledges the financial support of the German Federal Ministry of Education and Research (BMBF) under contract No. 01M3154A ("Abbildungsmethodiken für nanoelektrische Bauelemente").

REFERENCES

1. Chen, W., Carroll, J., Storm, G., Ivancich, R., Maloney, J., Maurin, O., and Souleillet, E., "Pellicle-induced reticle distortions: an experimental investigation," SPIE, Vol. 3546, pp. 167-172, 1998.
2. Röth, K.-D. and Struck, T., "Pellicle-induced distortions on photomasks," SPIE, Vol. 3412, pp. 440-446, 1998.
3. Wood, J., Eynon, B., and Kalk, F., "DUV pellicle quality assessment based on customer priorities," SPIE, Vol. 3546, pp. 422-428, 1998.
4. Cotte, E., Engelstad, R., Lovell, E., Shkel, Y., Eschbach, F., Shu, E., Tanzil, D., and Calhoun, R., "Distortions in advanced photomasks from soft pellicles," Microelectronic Engineering, Vol. 61-62, pp. 187-192, 2001.
5. Cotte, E., Engelstad, R., and Lovell, E., "Experimental and numerical studies of pellicle-induced photomask distortions," Proceedings of the Society for Experimental Mechanics, Vol. 61-62, pp. 187-192, 2002.
6. Cotte, E., Engelstad, R., Lovell, E., Tanzil, D., Eschbach, F., Korobko, Y., Fujita, M., and Nakagawa, H., "Effects of soft pellicle frame curvature and mounting process on pellicle-induced distortions in advanced photomasks," SPIE, Vol. 5040, pp. 1044-1054, 2003.
7. Fujita, M., Akiyama, M., Kondo, M, Nakagawa, H., Tanzil, D., Eschbach, F., Cotte, E., Engelstad, R., and Lovell, E., "Pellicle-induced distortions in advanced photomasks," SPIE, Vol. 4754, pp. 588-595, 2002.
8. Cotte, E., Engelstad, R., Lovell, E., Shkel, Y., Eschbach, F., Shu, E., Tanzil, D., and Calhoun, R., "Numerical and experimental studies of pellicle-induced photomasks distortions," SPIE, Vol. 4562, pp. 641-651, 2001.
9. Cotte, E., Engelstad, R., Lovell, E., Tanzil, D., Eschbach, F., and Shu, E., "Experimental and numerical studies of the effects of materials and attachment conditions on pellicle-induced distortions in advanced photomasks," SPIE, Vol. 4754, pp. 578-587, 2002.
10. Lutzenberger, C., Schilz, C., "Finite-element-analysis of photomask distortions", presented at the 4th International 157nm Symposium, Yokohama, Japan, 2003.
11. International Technology Roadmap for Semiconductors, 2003 edition, http://public.itrs.net.